

High endogenous calcium buffering in Purkinje cells from rat cerebellar slices

Leonardo Fierro and Isabel Llano*

Arbeitsgruppe Zelluläre Neurobiologie, Max-Planck-Institut für Biophysikalische Chemie, Am Fassberg, D37077 Göttingen, Germany

1. The ability of Purkinje cells to rapidly buffer depolarization-evoked intracellular calcium changes ($\Delta[\text{Ca}^{2+}]_i$) was estimated by titrating the endogenous buffer against incremental concentrations of the Ca^{2+} -sensitive dye fura-2.
2. In cells from 15-day-old rats, pulse-evoked $\Delta[\text{Ca}^{2+}]_i$ were stable during the loading with 0.5 mM fura-2 through the patch pipette. In cells from 6-day-old rats, $\Delta[\text{Ca}^{2+}]_i$ decreased by ~50% during equivalent experiments. This decrease was not related to changes in Ca^{2+} influx, since the integral of the Ca^{2+} currents remained constant throughout the recording.
3. Experiments with high fura-2 concentrations (1.75–3.5 mM) were performed in order to obtain for each cell the curve relating $\Delta[\text{Ca}^{2+}]_i$ to fura-2 concentration. From this relationship, values for the Ca^{2+} binding ratio (the ratio of buffer-bound Ca^{2+} changes over free Ca^{2+} changes) were calculated.
4. In Purkinje cells from 15-day-old rats, the Ca^{2+} binding ratio was ~2000, an order of magnitude larger than that of other neurones and neuroendocrine cells studied to date. This Ca^{2+} binding ratio was significantly smaller (~900) in Purkinje cells from 6-day-old rats.
5. We propose that the large Ca^{2+} binding ratio of Purkinje cells is related to the presence of large concentrations of Ca^{2+} binding proteins and that these cells regulate their ability to handle Ca_i^{2+} loads during development through changes in the concentration of Ca^{2+} binding proteins.

Rises in intracellular calcium concentration ($[\text{Ca}^{2+}]_i$) in cerebellar Purkinje cells occur as a result of Ca^{2+} influx through voltage-gated calcium channels (Llinás & Sugimori, 1980), Ca^{2+} release from inositol 1,4,5-trisphosphate-sensitive intracellular stores (Khodakhah & Ogden, 1995 and references therein) and Ca^{2+} -induced Ca^{2+} release (CICR) (Llano, DiPolo & Marty, 1994). $[\text{Ca}^{2+}]_i$ rises in Purkinje cells have been shown to have profound consequences for the efficacy of synapses they receive from both excitatory (Sakurai, 1990) and inhibitory inputs (reviewed by Marty & Llano, 1995). The effective Ca^{2+} concentration detected by Ca^{2+} -regulated intracellular components will depend, amongst other factors, on the ability of the Purkinje cell to rapidly buffer Ca_i^{2+} rises. The Ca^{2+} binding ratio, the ratio of buffer-bound Ca^{2+} changes to free Ca^{2+} changes, describes the effectiveness of endogenous buffers (Neher, 1995) and thus the capacity of the cell to handle Ca_i^{2+} loads. Purkinje cells are known to have large concentrations of endogenous buffers such as Ca^{2+} binding proteins (reviewed by Baimbridge, Celio & Rogers, 1992) which should endow them with a high Ca^{2+} binding ratio. Obtaining a reliable estimate of this parameter in Purkinje cells should give insights into their mechanisms for Ca^{2+} homeostasis and into

the functional role of Ca^{2+} binding proteins. Extensive theoretical analysis on the effects of exogenous buffers on Ca_i^{2+} dynamics has been performed (reviewed by Neher, 1995). Furthermore, it has been shown in neuroendocrine cells that the inclusion of Ca^{2+} -sensitive probes in the intracellular milieu can alter significantly the size, kinetics and spatial distribution of Ca_i^{2+} signals (Neher & Augustine, 1992; reviewed by Neher, 1995). Until recently, little attention has been paid to such problems in central nervous system preparations. Therefore, it is difficult to decide on their impact on the large body of data obtained with Ca^{2+} -sensitive probes in central neurones in general and in Purkinje cells in particular. The present work aims at providing an accurate estimate for the Ca^{2+} binding ratio in these cells.

METHODS

Sagittal 180 μm thick cerebellar slices were prepared as previously described (Llano, Marty, Armstrong & Konnerth, 1991) from rats which were decapitated following cervical dislocation. Animals from two age groups, 6 and 15 days old, were used in the present work. Tight-seal whole-cell recordings (WCR) were performed on

* To whom correspondence should be addressed.

Purkinje cells at room temperature (20–25 °C). The chamber was perfused at a rate of 1–1.5 ml min⁻¹ with a physiological saline (bicarbonate-buffered saline; BBS) which contained (mM): 125 NaCl, 2.5 KCl, 2 CaCl₂, 1 MgCl₂, 1.25 NaH₂PO₄, 26 NaHCO₃ and 10 glucose (pH of 7.4 when equilibrated with a mixture of 95% O₂–5% CO₂). Tetrodotoxin (200 nM; Sigma) and the GABA_A receptor antagonist bicuculline methochloride (10 μM; Tocris Cookson, Bristol, UK) were present in the extracellular solution throughout the experiments. Recording pipettes (borosilicate glass) had resistances of 2–2.5 MΩ; they were filled with a Cs⁺-containing internal solution (CsCl) of the following composition (mM): 150 CsCl, 4.6 MgCl₂, 10 Hepes acid, 0.4 GTP-Na and 4 ATP-Na₂ (pH adjusted to 7.35 with *N*-methyl-D-glucamine; osmolality was 295–300 mosmol kg⁻¹; stored at –20 °C). Salts and nucleotides for external and internal solutions were purchased from Sigma. The K⁺ salt of fura-2 (Molecular Probes) was included in the pipette solution at concentrations ranging from 0.5 to 3.5 mM. For fura-2 concentrations of 0.5 mM, fura-2 was prepared as a 10 mM stock, divided in 5 μl aliquots and kept at –20 °C. The internal solution was added daily to an aliquot to reach the final concentration. For higher concentrations of fura-2, 1 mg of fura-2 was dissolved directly in the internal solution and stored at –20 °C. No difference in the experimental results was observed as a result of the various batches of fura-2 used throughout this study.

Experiments were performed with an EPC-9 patch-clamp amplifier interfaced to a Macintosh Power PC computer via an ITC-16 interface. The Pulse software (Heka Electronics) was used for controlling the EPC-9 amplifier and the photometric set-up (see below) as well as for on-line data acquisition. Seal formation was achieved without prior cleaning of the neuronal surface, by maintaining a slight positive pressure in the pipette while approaching the cell. Under WCR, the membrane potential was held at –60 mV. The series resistance (*R_s*) was continuously monitored. Typical values for this parameter were 5–10 MΩ. Capacitance transient cancellation and *R_s* compensation (60–90% nominally) were performed as described (Llano *et al.* 1991).

Ca²⁺ measurements

A monochromator/photometric system from TILL Photonics (Germany) was used for excitation and monitoring of fluorescence signals. Excitation wavelengths (20 nm bandwidth) were alternated between 356 nm (the isosbestic point for fura-2) and 390 nm. The output of the monochromator was coupled to a Zeiss upright microscope via a quartz fibre optic and a UV condenser. A 10% transmission neutral-density filter (Omega Optical) was placed on the excitation pathway in order to avoid dye bleaching. Measurements were performed with a Zeiss ×63 water immersion lens (NA, 0.9). Fluorescence signals were collected after passing through an LP470 nm filter and measured with a photomultiplier from a square window of 20 μm width centred either on the cell soma or on the proximal dendritic arbor. This window was set by displacing a variable size pin-hole placed in front of the photomultiplier, while visually monitoring the area of choice with a back-illuminated video camera.

Prior to seal formation, the background fluorescence of the area chosen for recording upon excitation with 356 and 390 nm was measured. The cell-attached configuration was held until the background fluorescence at both wavelengths reached the value obtained prior to approach with the recording pipette. Following the establishment of WCR, voltage pulses to –10 mV were given at 30 s intervals for the first 5–6 min of loading, and at 1 min intervals thereafter while monitoring membrane current and the fluorescence signal resulting from 390 nm excitation. Mean values

of the fluorescence at the isosbestic point were obtained from 100 ms exposures to 356 nm illumination immediately preceding each voltage pulse.

Ca²⁺ was calculated according to Grynkiewicz, Poenie & Tsien (1985) after subtraction of background fluorescence. The parameters *R_{min}* (the fluorescence ratio in the absence of Ca²⁺), and *R_{max}* (the fluorescence ratio in the presence of saturating Ca²⁺) were 0.66 and 8, respectively. The ‘apparent’ dissociation constant of fura-2 (*K_d*) was 1.4 μM. (This constant is *K_d* × *S_{f2}*/*S₀₂*, in the notations of Grynkiewicz *et al.* 1985.) These values were derived from WCR of Purkinje cells performed with three calibrating solutions as described by Neher (1989). The composition of these solutions was as follows (mM): (a) for measurement of *R_{min}*: 120 CsCl, 10 Hepes acid, 10 BAPTA, 4.6 MgCl₂, 4 ATP-Na₂ and 0.4 GTP-Na; (b) for measurement of *R_{max}*: 130 CsCl, 10 Hepes acid and 10 CaCl₂; and (c) for calculation of *K_d*: 110 CsCl, 10 Hepes acid, 9.9 BAPTA, 6.6 CaCl₂, 4.6 MgCl₂, 4 ATP-Na₂ and 0.4 GTP-Na. For the three solutions pH was adjusted to 7.35 with CsOH, and the osmolality was 296 mosmol kg⁻¹. The Ca²⁺–BAPTA *K_d* was assumed to be 225 nM, after Zhou & Neher (1993). The fura-2 *K_d*, calculated as described by Zhou & Neher (1993), was 226 nM.

Determination of Ca²⁺ binding ratio

In the following analysis, based on the ‘added’ buffer approach introduced by Neher & Augustine (1992), it is considered that the incremental Ca²⁺ binding ratio (*κ_s*) is the ratio of the changes in Ca²⁺ bound to an endogenous buffer (S) ([CaS]) over free Ca²⁺ ([Ca²⁺]_i):

$$\kappa'_s = \frac{\Delta[\text{CaS}]}{\Delta[\text{Ca}^{2+}]_i} \quad (1)$$

In our experimental conditions, where an external Ca²⁺ buffer (F) is added to the cytosol, the total Ca²⁺ concentration change ($\Delta[\text{Ca}^{2+}]_T$) is given by:

$$\Delta[\text{Ca}^{2+}]_T = \Delta[\text{Ca}^{2+}]_i + \Delta[\text{CaF}] + \Delta[\text{CaS}] \quad (2)$$

A total Ca²⁺ binding ratio (*R*) may be defined by analogy to eqn (1) as:

$$R = \frac{\Delta[\text{Ca}^{2+}]_T}{\Delta[\text{Ca}^{2+}]_i} = \frac{[\text{Ca}^{2+}]_{Tp} - [\text{Ca}^{2+}]_{Tr}}{[\text{Ca}^{2+}]_{ip} - [\text{Ca}^{2+}]_{ir}} \quad (3)$$

where the indices p and r relate to the peak and resting conditions, respectively, for a depolarization-evoked increase in Ca²⁺. Combining eqns (1), (2) and (3) yields:

$$R = \kappa'_s + \kappa'_B + 1, \quad (4)$$

where *κ_B*, the incremental Ca²⁺ binding ratio for fura-2 (as defined in eqn (10) of Zhou & Neher, 1993) is given by:

$$\kappa'_B = \frac{\Delta[\text{CaF}]}{\Delta[\text{Ca}^{2+}]_i} = \frac{[\text{F}]/[\text{K}_d]}{(1 + [\text{Ca}^{2+}]_{ip}/[\text{K}_d])(1 + [\text{Ca}^{2+}]_{ir}/[\text{K}_d])} \quad (5)$$

where *K_d* is the dissociation constant of fura-2 for Ca²⁺. From eqn (3) and assuming constant $\Delta[\text{Ca}^{2+}]_T$ during the experiment, the ratio between the $\Delta[\text{Ca}^{2+}]_i$ measurements at two fura-2 concentrations is:

$$\frac{R_2}{R_1} = \frac{\Delta[\text{Ca}^{2+}]_{i1}}{\Delta[\text{Ca}^{2+}]_{i2}} \quad (6)$$

where indices 1 and 2 refer to the two fura-2 concentrations. Combining eqns (4), (5) and (6) yields an expression for *κ_s*:

$$\kappa'_s = \frac{(\Delta[\text{Ca}^{2+}]_{i2}(\kappa'_{B2} + 1)) - (\Delta[\text{Ca}^{2+}]_{i1}(\kappa'_{B1} + 1))}{(\Delta[\text{Ca}^{2+}]_{i1} - \Delta[\text{Ca}^{2+}]_{i2})} \quad (7)$$

In order to determine *κ_s* values from experiments in which $\Delta[\text{Ca}^{2+}]_i$

$$\Delta[\text{Ca}^{2+}]_i = -\frac{1}{2} \left(K_d + [\text{Ca}^{2+}]_{ir} + \frac{[\text{F}]K_d}{(K_d + [\text{Ca}^{2+}]_{ir})(1 + \kappa'_s)} - \Delta[\text{Ca}^{2+}]_{i0} \right) + \sqrt{\frac{1}{4} \left(K_d + [\text{Ca}^{2+}]_{ir} + \frac{[\text{F}]K_d}{(K_d + [\text{Ca}^{2+}]_{ir})(1 + \kappa'_s)} - \Delta[\text{Ca}^{2+}]_{i0} \right)^2 + \Delta[\text{Ca}^{2+}]_{i0}(K_d + [\text{Ca}^{2+}]_{ir})} \quad (8)$$

Equation (8)

was monitored in single cells as a function of the fura-2 concentration, eqn (7) was solved explicitly in terms of $\Delta[\text{Ca}^{2+}]_i$ and $[\text{F}]$, the experimental variables. This solution assumes that the resting Ca_i^{2+} ($[\text{Ca}^{2+}]_{ir}$) remains constant throughout the experiment, an assumption warranted by the data. The solution is given by eqn (8). In eqn (8), $\Delta[\text{Ca}^{2+}]_{i0}$ is the extrapolated value of $\Delta[\text{Ca}^{2+}]_i$ at zero fura-2 concentration. Equation (8) was used for estimating κ'_s and $\Delta[\text{Ca}^{2+}]_{i0}$ values from each experiment in cells loaded with high fura-2 concentration.

Statistical data are presented as means \pm S.E.M.

RESULTS

In previous work, it was shown that depolarization-induced Ca_i^{2+} signals are similar in Purkinje cells dialysed with 50–125 μM and with 500 μM fura-2 (Llano *et al.* 1994). We have now extended this analysis by performing experiments in which Ca_i^{2+} transients elicited by 40 ms depolarizations to -10 mV were monitored in Purkinje cells, at high concentrations of fura-2 (0.5–3.5 mM; to be given explicitly for each set of experiments) diffused from the pipette solution into the cytosol. The duration of the voltage step was chosen to avoid entering the range of Ca_i^{2+} levels in which CICR takes place in Purkinje cells (Llano *et al.* 1994).

The first series of experiments was carried out with 0.5 mM fura-2, in slices prepared from 15-day-old rats. Typical examples of the pulse-evoked Ca_i^{2+} transients at two different times in WCR are shown in Fig. 1, where panels *A* and *B* correspond to somatic and dendritic recordings of the fluorescence signals, respectively. In both cases, the time course as well as the magnitude of the pulse-evoked Ca_i^{2+} transients are quite similar in the early (upper traces) and later (lower traces) periods of the WCR trace, indicating that 0.5 mM fura-2 leads to little attenuation of the Ca_i^{2+} signals. Pooled data on the effect of 0.5 mM fura-2 from ten somatic recordings and six dendritic recordings are shown in Fig. 2 (see Discussion).

The interpretation of the effects of fura-2 loading on Ca_i^{2+} rises could be complicated if fura-2 binds to cytoplasmic components as shown in skeletal muscle (Baylor & Hollingworth, 1988) and cardiac cells (Blatter & Wier, 1990) or if it is extruded by active transport systems, as reported for macrophages (Di Virgilio, Steinberg, Swanson & Silverstein, 1988). As discussed by Neher (1995), binding of Ca^{2+} -sensitive dyes to cytoplasmic proteins seems to be a particular property of muscle, where the dye's dissociation constant *in vivo* differs by a factor of 4 from that found *in vitro* (Baylor & Hollingworth, 1988). In our case, the fura-2

K_d calculated from calibrations in Purkinje cells (see Methods) was close to *in vitro* values, as has been described for chromaffin cells (Zhou & Neher, 1993), arguing against fura-2 binding to cytoplasmic components.

In order to test for possible extrusion of fura-2 from the cytoplasm by probenecid-sensitive active anion transport (Di Virgilio *et al.* 1988), probenecid (2.5 mM) was applied in the bath solution after a stable fura-2 concentration had been reached (data not shown). An increase in the 356 nm excited fluorescence after probenecid application was observed if R_s exceeded 10 M Ω , indicating the presence of probenecid-sensitive extrusion in Purkinje cells. However, the effect was negligible if R_s was less than 10 M Ω . Therefore, all experiments reported here used R_s values below 10 M Ω . The low activity of this anion transporter in our experiments may be attributed to the condition of room temperature which markedly decreases probenecid-sensitive extrusion (Malgaroli, Milani, Meldolesi & Pozzan, 1987).

In a second series of experiments, Purkinje cells from 15-day-old rats were dialysed with 3.5 mM fura-2, and studied following the same protocol described above for the lower fura-2 concentration. Figure 2 compares pooled data on the changes in depolarization-induced somatic and dendritic Ca_i^{2+} transients ($\Delta[\text{Ca}^{2+}]_i$) obtained from Purkinje cells from 15-day-old rats dialysed either with 0.5 mM (\square) or with 3.5 mM fura-2 (\bullet). The behaviour of $\Delta[\text{Ca}^{2+}]_i$ with time in WCR differed significantly depending on the amount of added exogenous buffer. In contrast to the stable magnitude of the depolarization-induced Ca_i^{2+} transients in cells dialysed with 0.5 mM fura-2, both somatic and dendritic signals declined with time during dialysis with 3.5 mM fura-2 resulting in mean values of $\Delta[\text{Ca}^{2+}]_i$ at times of stable fura-2 loading normalized to the values at the earliest time of recording of 0.3 ± 0.03 for somatic recordings ($n = 7$) and 0.16 ± 0.05 for dendritic recordings ($n = 4$). In the initial 3 min of WCR, basal Ca_i^{2+} levels were close in all four experimental groups (for soma: 21.5 ± 1.6 nM ($n = 10$) and 30.3 ± 4 nM ($n = 7$) with 0.5 and 3.5 mM fura-2, respectively; for dendrites: 10 ± 2 nM ($n = 6$) and 22.5 ± 5.8 nM ($n = 4$) with 0.5 and 3.5 mM fura-2, respectively). The basal level did not show appreciable changes with time in WCR (mean values for the same cells at 15–17 min of WCR were for soma: 13.9 ± 1.2 and 20.4 ± 5.1 nM with 0.5 and 3.5 mM fura-2, respectively; and for dendrites: 9 ± 1.2 and 30.3 ± 8.1 nM with 0.5 and 3.5 mM fura-2, respectively). Likewise, the $\Delta[\text{Ca}^{2+}]_i$ values at early times in WCR was similar for both fura-2

concentrations tested, their absolute magnitude being approximately 7-fold larger in dendrites (156 ± 44 nM, $n = 6$ for the 0.5 mM group; 223 ± 56 nM, $n = 4$ for the 3.5 mM group) than in the soma (32 ± 5 nM, $n = 10$ in the 0.5 mM group; 22 ± 3 , $n = 7$ for the 3.5 mM group).

Before advancing a quantitative analysis of the data presented above in terms of the ability of the Purkinje cell's endogenous buffers to bind Ca^{2+} , the question arises as to whether the observed decline of $\Delta[\text{Ca}^{2+}]_i$ in cells loaded with 3.5 mM fura-2 is due to the effect of added exogenous buffer

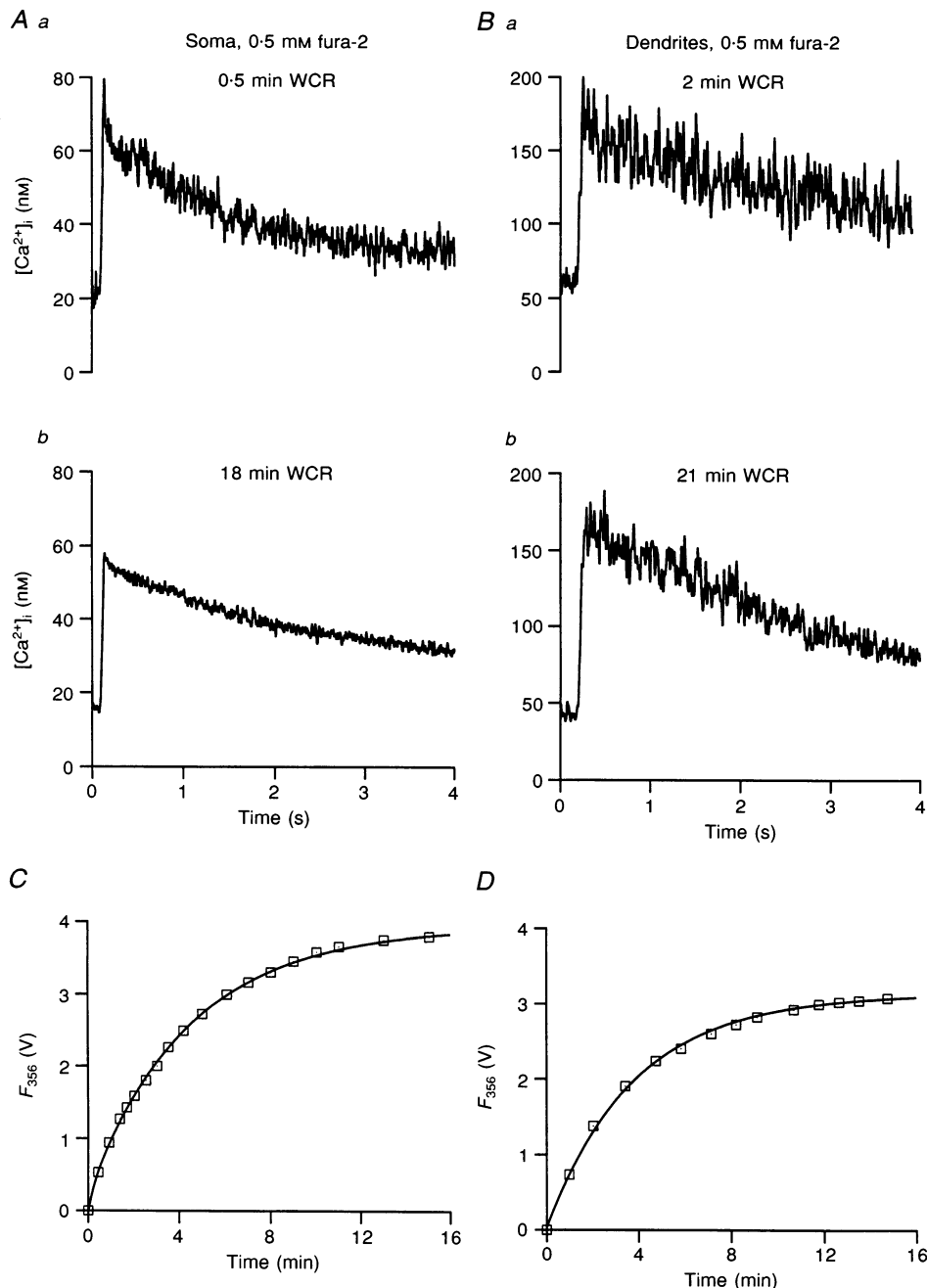


Figure 1. Lack of effect of 0.5 mM fura-2 in somatic and dendritic Ca_i^{2+} transients of Purkinje cells from 15-day-old rats

A, somatic Ca_i^{2+} transients evoked by a 40 ms pulse to -10 mV at 0.5 min (*a*) and 18 min (*b*) after establishment of whole-cell recording (WCR). *B*, dendritic Ca_i^{2+} transients evoked in a different cell by a 40 ms pulse to -10 mV, at 2 min (*a*) and 21 min (*b*) in WCR. In both cases, the pipette solution contained 0.5 mM fura-2. In this and subsequent experiments, the holding potential was -60 mV. *C* and *D* illustrate the loading curves for fura-2 for the 2 cells shown in *A* and *B*; the ordinate corresponds to the fluorescence signal upon 356 nm excitation (F_{356}). The experimental points have been fitted by double-exponential functions. Fitting parameters for the time constants (τ) and the amplitude coefficients (A) were: τ_a , 18 s; A_a , 0.25; τ_b , 4.4 min; A_b , 3.7 in *C*; and τ_a , 2.7 min; A_a , 2.3; τ_b , 15 min; A_b , 1.4 in *D*.

or to a time-dependent decline in Ca^{2+} influx. This point cannot be easily tested in Purkinje cells from 15-day-old rats, since the time constant for changing the membrane potential during a voltage step is slow compared with the gating kinetics of Ca^{2+} channels, rendering the recording of well-behaved Ca^{2+} currents impossible. The problem is circumvented in Purkinje cells from younger rats (less than 9 days old), where passive electrical properties (as inferred from the single-exponential nature of the capacitive transients) can be approximated well by a single R-C circuit with a time constant of the order of 0.4 ms, corresponding to membrane input capacitance of the order of 70 pF. In these cells, after appropriate capacitive cancellation and R_s compensation, the voltage-clamp time constant is less than 100 μs , thus allowing a faithful recording of voltage-gated Ca^{2+} currents (see Llano *et al.* 1994 and Fig. 3A).

Fura-2 loading experiments were performed in Purkinje cells from 6-day-old animals with the purposes of testing for (a) the stability of Ca^{2+} currents during the long recording times used in the fura-2 loading experiments and (b) developmental changes in κ'_s . An example of these experiments from a cell dialysed with 1.75 mM fura-2 is illustrated by Fig. 3. Traces in Fig. 3A show the Ca^{2+} currents and the corresponding somatic Ca_i^{2+} transient recorded at 1 and 8 min of WCR. Figure 3B shows plots for the same cell of $\Delta[\text{Ca}^{2+}]_i$ and of the integral of the Ca^{2+} current ($\int I_{\text{Ca}}$) as a function of time. $\int I_{\text{Ca}}$ was very stable during WCR. On average, the ratio of $\int I_{\text{Ca}}$ at times of maximum loading (9–13 min WCR) to that at early WCR (0.5–1.1 min) was 0.88 ± 0.05 ($n = 5$). Mean values of $\int I_{\text{Ca}}$ were 221 ± 43 pC for early WCR times and 194 ± 41 pC at maximum fura-2 loading times. No difference was observed either in the absolute magnitude of $\int I_{\text{Ca}}$ or in its stability

during WCR depending on the amount of fura-2 used in the recordings (0.5–3.5 mM, see data below). These results validate the use of fura-2 as an exogenous buffer for determinations of κ'_s in Purkinje cells.

In spite of the stability of the Ca^{2+} currents, and in contrast to the results derived from cells from 15-day-old rats, a significant decrease in somatic $\Delta[\text{Ca}^{2+}]_i$ as a function of time was observed in cells from 6-day-old rats when loaded with 0.5 mM fura-2. In five cells, the ratio of $\Delta[\text{Ca}^{2+}]_i$ in late times in WCR to that at early times in WCR was 0.53 ± 0.03 (the equivalent ratio for the 0.5 mM 15-day-old group was 1.41 ± 0.2 , $n = 10$). Figure 3C shows pooled results from this age group which present a clear time-dependent decrease in $\Delta[\text{Ca}^{2+}]_i$ as fura-2 (0.5 and 1.75 mM; see below) diffuses into the cells. Data has been normalized by the $\int I_{\text{Ca}}$. These results suggest that the κ'_s of Purkinje cells increases with age, which could have significant implications for the effective Ca^{2+} loads perceived by cytosolic constituents following Ca_i^{2+} rises. Also in support of this hypothesis is the fact that the magnitudes in depolarization-induced somatic $\Delta[\text{Ca}^{2+}]_i$ at early WCR times were significantly larger for slices from 6-day-old rats (144 ± 16 nM ($n = 5$) with 0.5 mM fura-2) than from the equivalent experiments in slices from 15-day-old rats (32 ± 4.9 nM ($n = 10$) with 0.5 mM fura-2).

In order to estimate κ'_s , experiments using either 3.5 mM (cells from 15-day-old rats) or 1.75 mM fura-2 (cells from 6-day-old rats) were further analysed. A lower fura-2 concentration was used in the younger cells since initial experiments done with 3.5 mM showed that such concentration was too high to allow accurate estimates of κ'_s to be performed. With 1.75 mM, it was found that the $\Delta[\text{Ca}^{2+}]_i$ decreased from 109 ± 22 nM at early times of

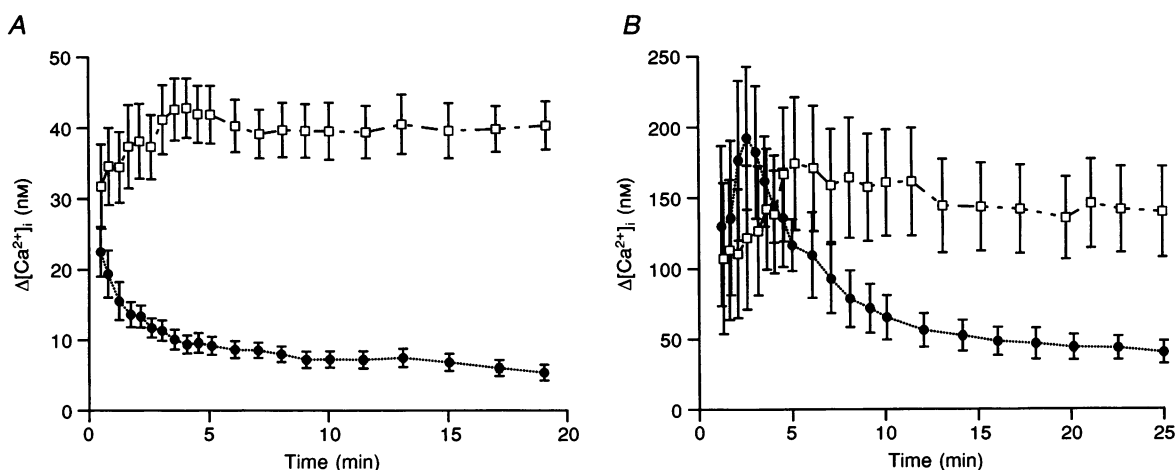


Figure 2. Comparison of the effect of 0.5 and 3.5 mM fura-2 in $[\text{Ca}^{2+}]_i$ transients of Purkinje cells from 15-day-old rats

A, temporal evolution of the somatic pulse-evoked $[\text{Ca}^{2+}]_i$ transients. In each experiment, the difference between peak Ca_i^{2+} and resting Ca_i^{2+} was calculated for each time point, to yield $\Delta[\text{Ca}^{2+}]_i$. The ordinate corresponds to the mean $\Delta[\text{Ca}^{2+}]_i$ from 10 cells loaded with 0.5 mM fura-2 (\square) and 7 cells loaded with 3.5 mM fura-2 (\bullet). *B*, temporal evolution of the dendritic pulse-evoked Ca_i^{2+} transients. Same experimental and analysis protocol as in *A*. $n = 6$ in 0.5 mM fura-2 and $n = 4$ in 3.5 mM fura-2.

WCR to 32 ± 7.6 nM at times of stable fura-2 loading ($n = 5$; see plot of pooled data in Fig. 3C). The average ratio of $\Delta[\text{Ca}^{2+}]_i$ at late to early times was 0.29 ± 0.02 , a value close to that obtained by loading Purkinje cells from 15-day-old rats with double the fura-2 concentration and thus in agreement with the suggestion that κ'_s is larger in the older cells.

The changes in $\Delta[\text{Ca}^{2+}]_i$ during the loading with fura-2 were used to calculate κ'_s according to eqn (8) (see Methods) from each experiment. Loading curves for the fluorescence signals elicited by 356 nm excitation were constructed for each cell and the data was translated into fura-2 concentration as a function of time, as shown by the examples in Fig. 4 (lower panels). The $\Delta[\text{Ca}^{2+}]_i$ was then plotted as a function of fura-2 concentration (Fig. 4, upper panels) and eqn (8) was fitted to the data in order to obtain values for κ'_s and for the extrapolated value of $\Delta[\text{Ca}^{2+}]_i$ at zero fura-2 concentration ($\Delta[\text{Ca}^{2+}]_{i0}$). The resulting fits are shown as continuous lines

in Fig. 4A and B. Following this procedure, κ'_s values of 919 ± 99 ($n = 5$) for the 6-day-old group and 2059 ± 482 ($n = 6$) for the 15-day-old group were obtained. Values for $\Delta[\text{Ca}^{2+}]_{i0}$ were 190 ± 14 and 58 ± 12 nM for the two groups, respectively. A rough estimate of κ'_s was also obtained from dendritic recordings of cells from 15-day-old rats, by comparing pooled values of $\Delta[\text{Ca}^{2+}]_i$ from several cells at times of stable loading with 0.5 (6 cells) and 3.5 mM (4 cells) fura-2, as in Llano *et al.* (1994). The estimated κ'_s was 2129, similar to that obtained from somatic recording at the same age.

DISCUSSION

The data presented here clearly indicate that the Ca^{2+} binding ratio of Purkinje cells is large compared with the estimates reported to date for a variety of mammalian neurones and neuroendocrine cells. Values for κ'_s in neuroendocrine cells range from 40 in adrenal chromaffin

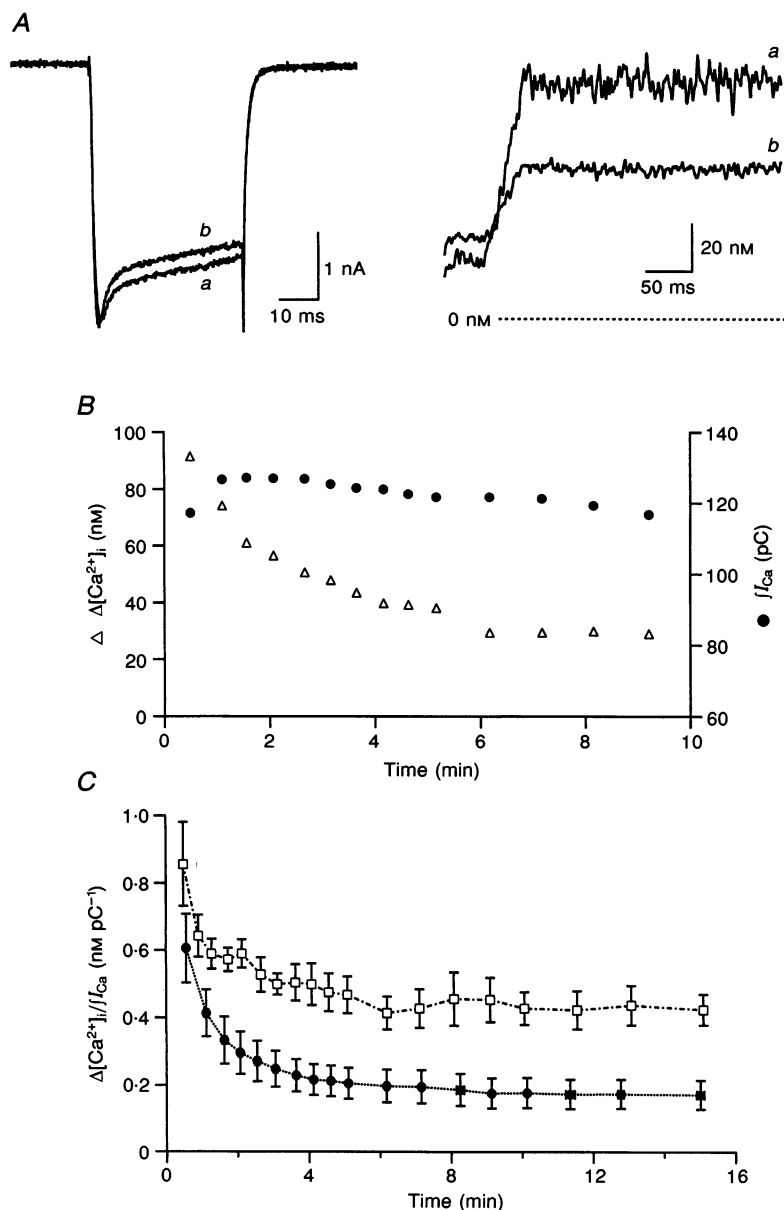


Figure 3. $[\text{Ca}^{2+}]_i$ transients and Ca^{2+} currents in young Purkinje cells

A, left panel shows the currents elicited by a 40 ms depolarizing pulse to -10 mV (a) and 8 min (b) of WCR from a cell from a 6-day-old rat. Leak and capacitive transients have been subtracted by a $P/4$ procedure. Pipette solution contained 1.75 mM fura-2. The right panel displays the corresponding somatic $[\text{Ca}^{2+}]_i$ transients. B, temporal evolution of $\Delta[\text{Ca}^{2+}]_i$ and Ca^{2+} currents. Open triangles represent the $\Delta[\text{Ca}^{2+}]_i$ as a function of time in WCR. Closed circles correspond to the integral of the Ca^{2+} current during the pulse. C, pooled data on somatic $\Delta[\text{Ca}^{2+}]_i$ from cells from a 6-day-old rat. The experimental and analysis protocol are as described for Fig. 2, with the exception that the ordinate represents the $\Delta[\text{Ca}^{2+}]_i$ divided by the Ca^{2+} current integral. Open squares correspond to pooled values from 5 cells (0.5 mM fura-2); closed circles correspond to 5 cells (1.75 mM fura-2).

cells (Zhou & Neher, 1993) to 100–130 in other preparations such as gonadotrophs (Tse, Tse & Hille, 1994), melanotrophs (Thomas, Surprenant & Almers, 1990) and GH3 cells (Lledo, Somasundaram, Morton, Emson & Mason, 1992). Evidence for low κ'_s in mammalian neurones stems from the changes produced by the addition of exogenous buffer in calcium transients and calcium-regulated electrical signals recorded from soma, dendrites and presynaptic terminals in a variety of preparations (reviewed by Regehr & Tank, 1994; Borst, Helmchen & Sakmann, 1995; Regehr & Atluri, 1995). Using the addition of exogenous buffer to estimate κ'_s , values of ~ 174 were obtained for neurohypophysial nerve endings (Stuenkel, 1994), and of ~ 126 for neurones from the nucleus basalis (Tatsumi & Katayama, 1993). Recently, Helmchen, Imoto & Sakmann (1996) reported κ'_s values in the range of 100–135 for cortical layer V pyramidal cells and of 168–207 for hippocampal CA1 pyramidal cells. For Purkinje cells at comparable ages, we find a value an order of magnitude higher.

At the source of the striking contrast between Purkinje cells and other neuronal types may be the finding, derived from a large number of immunocytochemical studies, that several

types of Ca^{2+} binding proteins are more abundant in GABA-releasing neurones, including Purkinje cells, than in glutamate-releasing neurones (reviewed by Baimbridge *et al.* 1992). Mean intracellular concentrations of parvalbumin of $45 \mu\text{M}$ have been reported for the cerebellar cortex (Plogmann & Celio, 1993) and estimates for the concentration of this protein in Purkinje cells are in the order of 50–100 μM for soma and dendrites and as high as 1 mM for their axons (Kosaka, Kosaka, Nakayama, Hunziker & Heizmann, 1993). Other Ca^{2+} binding proteins such as calbindin $\text{D}_{28\text{k}}$ and calcineurin are also known to be abundant in Purkinje cells (Heizmann & Hunziker, 1991). Although quantitative data on their intracellular concentration is not available, it has been suggested that calbindin $\text{D}_{28\text{k}}$ is present at still higher concentrations than parvalbumin. If we assume that, at 15 days old, the total κ'_s of 2000 is dominated by parvalbumin and calbindin $\text{D}_{28\text{k}}$, we can obtain an upper limit for the concentration of calbindin $\text{D}_{28\text{k}}$ in Purkinje cells. Taking the parvalbumin concentration to be 100 μM , its K_d for Ca^{2+} as 0.6 μM and two Ca^{2+} binding sites per parvalbumin molecule, the contribution of parvalbumin to κ'_s would equal 330. If the remaining Ca^{2+}

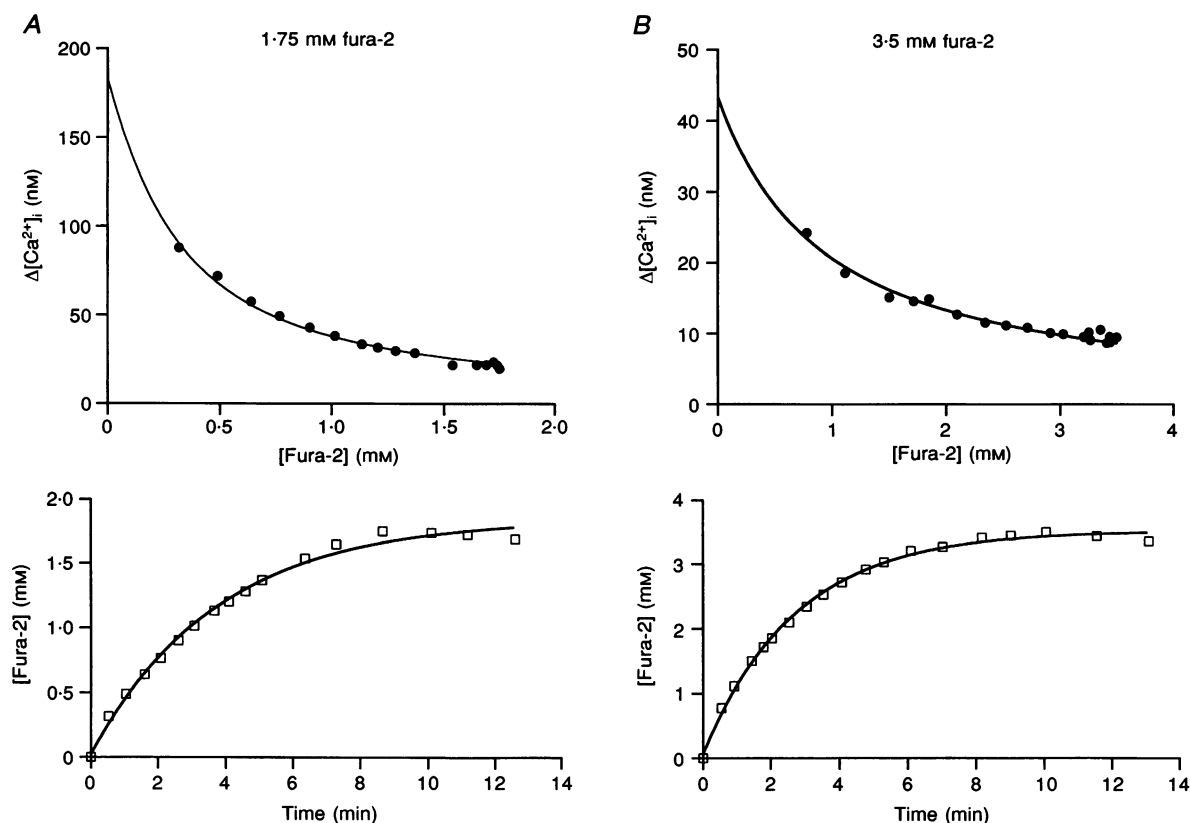


Figure 4. Estimation of Ca^{2+} binding ratio

Upper panels, plots of the $\Delta[\text{Ca}^{2+}]_i$ versus fura-2 concentration for a cell from a 6-day-old rat loaded with 1.75 mM fura-2 (A) and for a cell from a 15-day-old rat loaded with 3.5 mM fura-2 (B). The continuous lines correspond to the fitting of the experimental points to eqn (8), extrapolated to 0 fura-2 concentration. Fitting parameters were: κ'_s , 853; and $\Delta[\text{Ca}^{2+}]_{i0}$, 183 nM in A; and κ'_s , 2954; and $\Delta[\text{Ca}^{2+}]_{i0}$, 43 nM in B. Lower panels, plots of the fura-2 concentration as a function of WCR time. The continuous lines correspond to the fitting of the data points to a single-exponential function with time constant (τ) and amplitude coefficient (A) of: τ , 3.8 min; A, 1.82 mM in A; and τ , 2.7 min; A, 3.45 mM in B.

binding is given by calbindin D_{28k} , with a K_d for Ca^{2+} of $0.5 \mu M$ and four Ca^{2+} binding sites per calbindin molecule, the concentration of this protein would be around $210 \mu M$.

The second finding of the present work is that the capacity of Purkinje cells to buffer Ca^{2+}_i is subject to developmental changes. Of particular interest to this result is the finding that the amount of mRNA coding for calbindin as well as the number of expressed protein molecules, increases during the time window of the present study (Iacopino, Rhoten & Christakos, 1990; Kurobe, Inaguma, Shinohara, Semba, Inagaki & Kato, 1992). Peak levels of calbindin and calretinin expression are reached around 60 days postnatal, and remain high up to old age (Villa, Podini, Panzeri, Racchetti & Meldolesi, 1994). Data on developmental changes in parvalbumin are not available for the cerebellar cortex, although there is evidence for an age-dependent increase of this protein in the monkey striated cortex (Hendrickson, Van Brederode, Mulligan & Celio, 1991). These results and the data here reported suggest that rat cerebellar Purkinje cells regulate their ability to handle Ca^{2+}_i loads during development by increasing the expression of calbindin D_{28k} and perhaps that of other Ca^{2+} binding proteins.

The role of these proteins in Ca^{2+}_i buffering is supported by a variety of biochemical and electrophysiological data (Table II, Schäfer & Heizmann, 1996 and references therein). The amplitude and decay time course of depolarization-evoked $[Ca^{2+}]_i$ transients are significantly altered in sensory neurones by the addition, via patch pipettes, of calbindin D_{28k} and of parvalbumin (Chard, Bleakman, Christakos, Fullmer & Miller, 1993) and, in GH3 cells, by transfection with calbindin D_{28k} (Lledo *et al.* 1992). In the supraoptic nucleus, phasically firing neurones change their firing pattern from phasic to continuous upon dialysis with calbindin, whereas continuously firing neurones turn to phasic firing when dialysed with anti-calbindin antiserum (Li, Decavel & Hatton, 1995). In hair sacculus cells, high concentrations of Ca^{2+} binding proteins have been suggested to play a key role in the spatial buffering of Ca^{2+}_i signals, thereby regulating the encoding of sensory information (Roberts, 1994).

The exact role of the powerful Ca^{2+} buffering of Purkinje cells and its potential relation to the cellular changes which take place during early postnatal development remain to be determined. During the first three postnatal weeks Purkinje cells in rodents grow rapidly and develop their characteristic dendritic arborization. The entire cerebellar cortex undergoes intensive synaptogenesis, as numerous synaptic contacts are established onto Purkinje cells by excitatory and inhibitory afferents (Larramendi, 1969). The firing rate of Purkinje cells, studied *in vivo*, has been reported to increase throughout this period (Woodward, Hoffer & Lapham, 1969). Changes in ionic conductances are likely to accompany the growth and synaptogenesis of Purkinje cells. It has indeed been shown that 1 day after birth the spiking pattern of Purkinje cells is dominated by voltage-gated Na^+ currents, whereas voltage-gated Ca^{2+} conductances appear 3–4 days postnatal, paralleling the

development of dendritic processes (Llinás & Sugimori, 1979). It is tempting to speculate that the development of high Ca^{2+} -buffering capacity by Purkinje cells during the first two postnatal weeks might serve to handle increasing Ca^{2+} loads due to bombardment by newly formed excitatory synaptic contacts and the subsequent activation of voltage-gated Ca^{2+} channels.

- BAIMBRIDGE, K. G., CELIO, M. R. & ROGERS, J. H. (1992). Calcium-binding proteins in the nervous system. *Trends in Neurosciences* **15**, 303–308.
- BAYLOR, S. M. & HOLLINGWORTH, S. (1988). Fura-2 calcium transients in frog skeletal muscle fibres. *Journal of Physiology* **403**, 151–192.
- BLATTER, L. A. & WIER, W. G. (1990). Intracellular diffusion, binding, and compartmentalization of the fluorescent calcium indicators Indo-1 and Fura-2. *Biophysical Journal* **58**, 1491–1499.
- BORST, J. G. G., HELMCHEN, F. & SAKMANN, B. (1995). Pre- and postsynaptic whole-cell recordings in the medial nucleus of the trapezoid body of the rat. *Journal of Physiology* **489**, 825–840.
- CHARD, P., BLEAKMAN, D., CHRISTAKOS, S., FULLMER, C. S. & MILLER, R. J. (1993). Calcium buffering properties of calbindin D_{28k} and parvalbumin in rat sensory neurones. *Journal of Physiology* **472**, 341–357.
- DI VIRGILIO, F., STEINBERG, T. H., SWANSON, J. A. & SILVERSTEIN, S. C. (1988). Fura-2 secretion and sequestration in macrophages: A blocker of organic anion transport reveals that these processes occur via a membrane transport system for organic anions. *Journal of Immunology* **140**, 915–920.
- GRYNKIEWICZ, G., POENIE, M. & TSIEN, R. Y. (1985). A new generation of Ca^{2+} indicators with greatly improved probe properties. *Journal of Biological Chemistry* **260**, 3440–3450.
- HEIZMANN, C. W. & HUNZIKER, W. (1991). Intracellular calcium-binding proteins: more sites than insights. *Trends in Biochemical Sciences* **16**, 98–103.
- HELMCHEN, F., IMOTO, K. & SAKMANN, B. (1996). Ca^{2+} buffering and action potential-evoked Ca^{2+} signaling in dendrites of pyramidal neurons. *Biophysical Journal* **70**, 1069–1081.
- HENDRICKSON, A. E., VAN BREDERODE, J. F., MULLIGAN, K. A. & CELIO, M. R. (1991). Development of the calcium-binding proteins parvalbumin and calbindin in monkey striate cortex. *Journal of Comparative Neurology* **307**, 626–646.
- IACOPINO, A. M., RHOTEN, W. B. & CHRISTAKOS, S. (1990). Calcium binding protein (calbindin- D_{28k}) gene expression in the developing and aging mouse cerebellum. *Molecular Brain Research* **8**, 283–290.
- KHODAKHAH, K. & OGDEN, D. (1995). Fast activation and inactivation of inositol trisphosphate-evoked Ca^{2+} release in rat cerebellar Purkinje neurones. *Journal of Physiology* **487**, 343–358.
- KOSAKA, T., KOSAKA, K., NAKAYAMA, T., HUNZIKER, W. & HEIZMANN, C. W. (1993). Axons and axon terminals of cerebellar Purkinje cells and basket cells have higher levels of parvalbumin immunoreactivity than somata and dendrites: quantitative analysis by immunogold labeling. *Experimental Brain Research* **93**, 483–491.
- KUROBE, N., INAGUMA, Y., SHINOHARA, H., SEMBA, R., INAGAKI, T. & KATO, K. (1992). Developmental and age-dependent changes of 28-kDa calbindin-D in the central nervous tissue determined with a sensitive immunoassay method. *Journal of Neurochemistry* **58**, 128–134.

- LARRAMENDI, L. M. H. (1969). Analysis of synaptogenesis in the cerebellum of the mouse. In *Neurobiology of Cerebellar Evolution and Development*, ed. LLINÁS, R., pp. 803–843. American Medical Association, Chicago, USA.
- LI, Z., DECAVEL, C. & HATTON, G. I. (1995). Calbindin-D_{28k}: role in determining intrinsically generated firing patterns in rat supraoptic neurones. *Journal of Physiology* **488**, 601–608.
- LLANO, I., MARTY, A., ARMSTRONG, C. M. & KONNERTH, A. (1991). Synaptic- and agonist-induced excitatory currents of Purkinje cells in rat cerebellar slices. *Journal of Physiology* **434**, 183–213.
- LLANO, I., DIPOLO, R. & MARTY, A. (1994). Calcium-induced calcium release in cerebellar Purkinje cells. *Neuron* **12**, 663–673.
- LLEDO, P. M., SOMASUNDARAM, B., MORTON, A. J., EMSON, P. C. & WATSON, W. T. (1992). Stable transfection of calbindin D_{28k} into the GH3 cell line alters calcium currents and intracellular calcium homeostasis. *Neuron* **9**, 943–954.
- LLINÁS, R. & SUGIMORI, M. (1979). Calcium conductances in Purkinje cell dendrites: Their role in development and integration. *Progress in Brain Research* **51**, 323–334.
- LLINÁS, R. & SUGIMORI, M. (1980). Electrophysiological properties of *in vitro* Purkinje cell dendrites in mammalian cerebellar slices. *Journal of Physiology* **305**, 197–213.
- MALGAROLI, A., MILANI, D., MELDOLESI, J. & POZZAN, T. (1987). Fura-2 measurements of cytosolic free Ca²⁺ in monolayers and suspensions of various types of animal cells. *Journal of Cell Biology* **105**, 2145–2155.
- MARTY, A. & LLANO, I. (1995). Modulation of inhibitory synapses in the mammalian brain. *Current Opinion in Neurobiology* **5**, 335–341.
- NEHER, E. (1989). Combined Fura-2 and patch-clamp measurements in rat peritoneal mast cells. In *Neuromuscular Junction* **5**, ed. SELLIN, L. C., LIBELIUS, R. & THESLEFF, S., pp. 65–76. Elsevier, Amsterdam.
- NEHER, E. (1995). The use of fura-2 for estimating Ca buffers and Ca fluxes. *Neuropharmacology* **34**, 1423–1442.
- NEHER, E. & AUGUSTINE, G. J. (1992). Calcium gradients and buffers in bovine chromaffin cells. *Journal of Physiology* **450**, 273–301.
- PLOGMANN, D. & CELIO, M. R. (1993). Intracellular concentration of parvalbumin in nerve cells. *Brain Research* **600**, 273–279.
- REGHEHR, W. G. & ATLURI, P. P. (1995). Calcium transients in cerebellar granule cell presynaptic terminals. *Biophysical Journal* **68**, 2156–2170.
- REGHEHR, W. G. & TANK, D. W. (1994). Dendritic calcium dynamics. *Current Opinion in Neurobiology* **4**, 373–382.
- ROBERTS, W. M. (1994). Localization of calcium signals by a mobile calcium buffer in frog saccular hair cells. *Journal of Neuroscience* **14**, 3246–3262.
- SAKURAI, M. (1990). Calcium is an intracellular mediator of the climbing fiber in induction of cerebellar long-term depression. *Proceedings of the National Academy of Sciences of the USA* **87**, 3383–3385.
- SCHÄFER, B. W. & HEIZMANN, C. W. (1996). The S100 family of EF-hand calcium-binding proteins: functions and pathology. *Trends in Biochemical Sciences* **21**, 134–140.
- STUENKEL, E. L. (1994). Regulation of intracellular calcium and calcium buffering properties of rat isolated neurohypophysial nerve endings. *Journal of Physiology* **481**, 251–271.
- TATSUMI, H. & KATAYAMA, Y. (1993). Regulation of the intracellular free calcium concentration in acutely dissociated neurones from rat nucleus basalis. *Journal of Physiology* **464**, 165–181.
- THOMAS, P., SURPRENANT, A. & ALMERS, W. (1990). Cytosolic Ca²⁺, exocytosis and endocytosis in single melanotrophs of the rat pituitary. *Neuron* **5**, 723–733.
- TSE, A., TSE, F. W. & HILLE, B. (1994). Calcium homeostasis in identified rat gonadotrophs. *Journal of Physiology* **477**, 511–525.
- VILLA, A., PODINI, P., PANZERI, M. C., RACCHETTI, G. & MELDOLESI, J. (1994). Cytosolic Ca²⁺ binding proteins during rat brain ageing: loss of calbindin and calretinin in the hippocampus, with no change in the cerebellum. *European Journal of Neuroscience* **6**, 1491–1499.
- WOODWARD, D. J., HOFFER, B. J. & LAPHAM, L. W. (1969). Correlative survey of electrophysiological, neuropharmacological, and histochemical aspects of cerebellar maturation in rat. In *Neurobiology of Cerebellar Evolution and Development*, ed. LLINÁS, R., pp. 725–747. American Medical Association, Chicago, USA.
- ZHOU, Z. & NEHER, E. (1993). Mobile and immobile calcium buffers in bovine adrenal chromaffin cells. *Journal of Physiology* **469**, 245–273.

Acknowledgements

We thank Dr A. Marty for invaluable discussions throughout the course of this study and Professor E. Neher for his comments on the manuscript. We are grateful to C. Pouzat and C. Auger for aid on mathematical derivations and analysis routines. This work was supported by the Max-Planck-Gesellschaft, by grants from the Deutsche Forschungsgemeinschaft, the Hildegard Doerenkamp-Gerhard Zbinden Foundation and a doctoral fellowship from the Colombian Institute for the Development of Science and Technology (COLCIENCIAS) to Dr L. Fierro.

Author's email address

I. Llano: ILLANO@GWDG.DE

Received 22 April 1996; accepted 18 July 1996.